

# How chaotic are the pion sources in Au+Au collisions at $\sqrt{s_{\text{NN}}} = 130$ GeV?

Kenji Morita,<sup>1,\*</sup> Shin Muroya,<sup>2,†</sup> and Hiroki Nakamura<sup>1,‡</sup>

<sup>1</sup>*Department of Physics, Waseda University, Tokyo 169-8555, Japan*

<sup>2</sup>*Tokuyama Women's College, Shunan, Yamaguchi 745-8511, Japan*

(Dated: January 28, 2020)

We analyze consistently the two-pion correlation function and the three-pion correlation function of 130A GeV Au+Au collisions at the RHIC. The effect of long-lived resonances on the chaoticity in the two-pion correlation function is estimated based on the statistical model. Three kinds of partial coherent models are investigated. Any of the three models indicates that pions are emitted from the mixture of a chaotic source and coherent sources in the 130A GeV Au+Au collisions.

PACS numbers: 25.75.Gz

Pion interferometry is one of the most powerful tools in relativistic heavy ion physics. The fact that two-boson intensity correlation functions provide information on the geometry of particle sources is known as Hanbury Brown-Twiss (HBT) effect. The two-pion correlation function  $C_2(\mathbf{p}_1, \mathbf{p}_2)$  has been extensively analyzed for exploring space-time structures of the collision dynamics [1]. The HBT effect is based on an assumption of a chaotic source, *i.e.*, particles are emitted with relatively random phases. The chaoticity index in the two-particle correlation function  $\lambda$  is defined as the two-pion correlation strength  $\lambda = C_2(\mathbf{p}, \mathbf{p}) - 1$ , and becomes unity for the chaotic source and vanishes for the coherent ones. Thermal emission is naturally accepted as a perfect chaotic source [2, 3]

but non-thermal components need not to be perfectly chaotic. If a disoriented chiral condensation (DCC) region is produced, the domain can decay into coherent pions. Therefore, the chaoticity index  $\lambda$  is an important parameter to understand multiple particle production. However, experimental data are not so simple; even for the chaotic source, the chaoticity can be reduced by some other effects such as long-lived resonances [4, 5, 6, 7, 8].

As an alternative tool to investigate particle sources, the three-particle correlation function has also been available [9, 10, 11, 12]. As for the chaoticity of the sources, the three-particle correlation is a more promising tool than the two-particle correlation because long-lived resonances do not affect a normalized three-pion correlator,

$$r_3(\mathbf{p}_1, \mathbf{p}_2, \mathbf{p}_3) = \frac{[C_3(\mathbf{p}_1, \mathbf{p}_2, \mathbf{p}_3) - 1] - [C_2(\mathbf{p}_1, \mathbf{p}_2) - 1] - [C_2(\mathbf{p}_2, \mathbf{p}_3) - 1] - [C_2(\mathbf{p}_3, \mathbf{p}_1) - 1]}{\sqrt{[C_2(\mathbf{p}_1, \mathbf{p}_2) - 1][C_2(\mathbf{p}_2, \mathbf{p}_3) - 1][C_2(\mathbf{p}_3, \mathbf{p}_1) - 1]}}. \quad (1)$$

The index of the chaoticity in the three-pion correlator is a weight factor  $\omega = r_3(\mathbf{p}, \mathbf{p}, \mathbf{p})/2$  that becomes unity

for the chaotic source. The three-pion correlator used in the present experiments is slightly different from Eq.(1):

$$r_3(Q_3) = \frac{[C_3(Q_3) - 1] - [C_2(Q_{12}) - 1] - [C_2(Q_{23}) - 1] - [C_2(Q_{31}) - 1]}{\sqrt{[C_2(Q_{12}) - 1][C_2(Q_{23}) - 1][C_2(Q_{31}) - 1]}}. \quad (2)$$

where  $Q_{ij} = -(p_i - p_j)^2$  and  $Q_3 = \sqrt{Q_{12}^2 + Q_{23}^2 + Q_{31}^2}$ , and  $\omega$  is defined as  $r_3(0)/2$ . In both definitions,  $\omega$  are expected to become the same at small  $Q_3$ .

In this letter, we present an analysis of both the three- and the two-pion correlation data measured by the STAR collaboration [13] for central events in Au+Au collisions at 130A GeV. The STAR collaboration, adopting a partial coherent model for the pion source, concludes that about 80% of pions are emitted from the chaotic source in

such collisions [13]. However, this is the result of three-pion data only and the obtained value seems to be inconsistent with the  $\lambda$  of the two-pion correlation. This apparent discrepancy does not directly mean that the analysis is inconsistent. As noted in the Ref. [13], the chaoticity  $\lambda$  in the two-pion correlation can be affected by long-lived resonances. More refined and consistent analyses on both three- and two-pion correlation functions are the subject of this letter. In the following, we first

make correction to the two-pion correlation function for the long-lived resonance decay contributions. After that, we investigate the chaoticity of the pion sources based on the three kinds of the partial coherent source models.

Let us start with giving a brief explanation of the models. Model I is the partial coherent model [10] of which the solitary parameter  $\varepsilon_{\text{pc}}$  is the ratio of the particle number emitted from the chaotic source to that from the total. The chaoticity  $\lambda$  and the weight factor  $\omega$  are given as

$$\lambda = \varepsilon_{\text{pc}}(2 - \varepsilon_{\text{pc}}), \quad \omega = \sqrt{\varepsilon_{\text{pc}}} \frac{3 - 2\varepsilon_{\text{pc}}}{(2 - \varepsilon_{\text{pc}})^{3/2}}. \quad (3)$$

Model II is a multicoherent source model [12] in which the source is composed of a large number of the similar coherent sources. The  $\lambda$  and  $\omega$  are given as

$$\lambda = \frac{\alpha_m}{\alpha_m + 1}, \quad \omega = \frac{1}{2} \frac{2\alpha_m^2 + 2\alpha_m + 3}{\alpha_m^2 + 3\alpha_m + 1} \sqrt{\frac{\alpha_m + 1}{\alpha_m}}, \quad (4)$$

where  $\alpha_m$  corresponds to the mean number of coherent sources which obeys the Poisson distribution. Note that above two models contain single parameter only ( $\varepsilon_{\text{pc}}$  for the model I and  $\alpha_m$  for the model II) for two quantities, the chaoticity  $\lambda$  and the weight factor  $\omega$ . Model III is a mixture of above two models [12] and has already been applied to the SPS data by one of the present authors (H.N.) [14]. This model contains two parameters which are related to the  $\lambda$  and  $\omega$  as

$$\lambda = \frac{\alpha}{\alpha + (1 - \varepsilon)^2}, \quad (5)$$

$$\omega = \frac{2\alpha^2 + 2\alpha(1 - \varepsilon)^2 + 3(1 - \varepsilon)^3(1 - 2\varepsilon)}{2[\alpha^2 + 3\alpha(1 - \varepsilon)^2 + (1 - \varepsilon)^3]} \times \sqrt{\frac{\alpha + (1 - \varepsilon)^2}{\alpha}}, \quad (6)$$

where  $\varepsilon$  and  $\alpha$  are the ratio of the number of the particles from the chaotic source to that of the total and the mean number of coherent sources, respectively.

Putting  $\lambda$  and  $\omega$  of the experimental data into above equations, we can obtain the parameters of the models, the  $\varepsilon$ 's and the  $\alpha$ 's. In the model I and II,  $\lambda$  and  $\omega$  must provide consistent values for the single parameter  $\varepsilon_{\text{pc}}$  or  $\alpha_m$ . As we noted in the previous page, the STAR group analysis of the weight factor  $\omega$  in the central Au+Au collisions at  $\sqrt{s_{NN}} = 130$  GeV based on the model I indicates  $\varepsilon_{\text{pc}} \simeq 0.8$  which corresponds to  $\lambda \simeq 0.94$  [13]. Such a large  $\lambda$  seems to contradict the two-particle correlation data. But, we shall make correction of the long-lived resonances for the two-pion correlation function before proceeding to the conclusive calculations of Eqs.(3)-(6).

The presence of long-lived resonances which decay into pions causes the apparent reduction of the chaoticity in the two-pion correlation function. The reduction factor

$\lambda^{\text{eff}}$  is related to a fraction of pions from long-lived resonances as [6],

$$\sqrt{\lambda^{\text{eff}}} = 1 - \frac{N_\pi^r}{N_\pi}, \quad (7)$$

with  $N_\pi$  being the number of total emitted pions and  $N_\pi^r$  being the number of pions from long-lived resonances, respectively. We estimate the fraction of the  $\pi^-$  originating from the resonances with the help of the statistical model. According to the recent analyses, the statistical model provides a simple and good description of the particle yields of the RHIC experiments [15, 16]. We take account of the resonances up to  $\Sigma^*(1385)$ , in accordance with Ref. [8]. We treat  $K_s^0, \eta, \eta', \phi, \Lambda, \Sigma$  and  $\Xi$  as the long-lived resonances of which width is smaller than 5 MeV. Heavier resonances will be negligible because their contributions are thermally suppressed. The thermodynamical parameters are determined by a  $\chi^2$  fitting to the experimental data. From the fit, we get  $T = 158 \pm 9$  MeV and  $\mu_B = 36 \pm 6$  MeV with  $\chi^2/\text{dof} = 2.4/5$  [17]. The ratio of the particle  $i$  to the particle  $j$  can be calculated through the number densities at the local rest frame [18]. Then, the true chaoticity  $\lambda^{\text{true}}$  which is characterized by the partial coherence of the source is estimated as  $\lambda^{\text{true}} = \lambda^{\text{exp}}/\lambda^{\text{eff}}$  with use of Eqs. (7). The STAR collaboration measures [19]  $\lambda^{\text{exp}}$  for three transverse momentum bins. Since the transverse momentum dependence of the  $\lambda^{\text{exp}}$  agrees with expectations from Eq.(7) [8], the  $\lambda^{\text{exp}}$  for the whole momentum range can be calculated by averaging  $\lambda_i^{\text{exp}}$  with taking a squared number of pions as a weight,

$$\bar{\lambda}^{\text{exp}} = \frac{\sum_{i=1}^3 \lambda_i^{\text{exp}} \int_{i\text{-th bin}} k_t dk_t (dN/k_t dk_t)^2}{\sum_{i=1}^3 \int_{i\text{-th bin}} k_t dk_t (dN/k_t dk_t)^2}, \quad (8)$$

where  $\lambda_i^{\text{exp}}$  and  $dN/k_t dk_t$  denote the measured chaoticity in the  $i$ -th bin and the pion transverse momentum distributions, respectively. In the calculation of Eq.(8), we use a result of Bose-Einstein fit to the pion spectra by the STAR collaboration [20]. As a result of Eq.(8), we get  $\bar{\lambda}^{\text{exp}} = 0.57 \pm 0.06$ . Combining  $\lambda^{\text{eff}}$  obtained from the statistical model calculation, we finally obtain  $\lambda^{\text{true}} = 0.93 \pm 0.08$  for the present parameter region.

In order to obtain the weight factor  $\omega$ , we have to extrapolate  $r_3(Q_3)$  in Eq.(2) to  $Q_3 = 0$ . Because  $r_3(Q_3)$  is constructed by  $C_2(Q_{\text{inv}}) - 1$  and  $C_3(Q_3) - 1$  [Eq.(2)], we need to establish the functional form of  $C_2(Q_{\text{inv}})$  and  $C_3(Q_3)$  so as to reproduce the experimental data (Figs. 1 and 2). Although quadratic and quartic fits are used in Ref. [13], we adopt an alternative approach because the  $Q_3$  dependence of  $r_3$  may be more complicated [11] and the quadratic and quartic fitting tends to lead to the overestimated weight factor. In the following, we treat a set of  $\pi^-$  data measured in the lowest momentum bin for the highest multiplicity events [13]. We construct the  $C_2$  and  $C_3$  from simple source functions with a set of

parameters, which is determined by minimizing  $\chi^2$  with respect to the experimental data. For simplicity, we used a spherically symmetric source with simultaneous emission,  $F_{ij} = f_{ij}(|\mathbf{q}_{ij}|)e^{i(E_i-E_j)t_0}$ , where the exponential term corresponds to emissions at a constant time  $t_0$ . For the spacial part, we try a gaussian, an exponential, and a function in terms of  $\cosh$ , which becomes quadratic at small  $|\mathbf{q}|$  and exponential at large  $|\mathbf{q}|$ ,

$$f_{1,ij}(|\mathbf{q}_{ij}|) = \exp(-R^2|\mathbf{q}_{ij}|^2/2), \quad (9)$$

$$f_{2,ij}(|\mathbf{q}_{ij}|) = \exp(-R|\mathbf{q}_{ij}|/2), \quad (10)$$

$$f_{3,ij}(|\mathbf{q}_{ij}|) = \frac{1}{\sqrt{\cosh(-R|\mathbf{q}_{ij}|)}}, \quad (11)$$

where  $\mathbf{q}_{ij} = \mathbf{p}_i - \mathbf{p}_j$  and  $R$  is the size parameter. Correlation functions are then calculated through

$$C_2(\mathbf{p}_1, \mathbf{p}_2) = 1 + \lambda \frac{f_{12}^2}{f_{11}f_{22}}, \quad (12)$$

and

$$C_3(\mathbf{p}_1, \mathbf{p}_2, \mathbf{p}_3) = 1 + \nu \left( \sum_{(i,j)} \frac{f_{ij}^2}{f_{ii}f_{jj}} + 2 \frac{f_{12}f_{23}f_{31}}{f_{11}f_{22}f_{33}} \right), \quad (13)$$

where  $\lambda$  and  $\nu$  are phenomenological adjustable parameters accounting for non-trivial coherence effects and  $\sum_{(i,j)}$  is summation over  $(i,j) = (1,2), (2,3), (3,2)$ . The parameter  $R$ ,  $\lambda$  and  $\nu$  are determined by a simultaneous  $\chi^2$  fitting to both of  $C_2(Q_{\text{inv}})$  and  $C_3(Q_3)$ . The three-particle correlator  $r_3(Q_3)/2$  is then obtained by separate projections of the numerator and the denominator in Eq.(2) onto the single variable  $Q_3$  [21]. The results are shown in Figs. 1, 2, and 3 and summarized in Table. I.

TABLE I: Results of the  $\chi^2$  fitting to  $C_2$  and  $C_3$

$f( \mathbf{q} )$	$R$ [fm]	$\lambda$	$\nu$	$\chi^2/\text{dof}$	$\omega$
$f_1$	$7.0 \pm 0.07$	$0.54 \pm 0.01$	$0.48 \pm 0.01$	110/30	$0.958 \pm 0.09$
$f_2$	$14.4 \pm 0.2$	$1.18 \pm 0.03$	$1.08 \pm 0.03$	79.7/30	$0.736 \pm 0.09$
$f_3$	$15.2 \pm 0.2$	$0.71 \pm 0.01$	$0.64 \pm 0.02$	15.8/30	$0.872 \pm 0.097$

The results show failures of the gaussian [Eq.(9)] and the exponential [Eq.(10)] fittings. Figures 1 and 2 might be well but the values of  $\chi^2/\text{dof}$  are larger than the  $\cosh$  source function case. Furthermore, the disagreement in  $r_3(Q_3)$  of the exponential (gaussian) case shows over(under-)estimation of  $C_2$  at small  $Q_{\text{inv}}$  extrapolation. On the other hand, the  $\cosh$  source function [Eq.(11)] results in an excellent agreement with the experimental data. The deviation in Fig. 3 at larger  $Q_3^2$  is not significant. Since both of the numerator and the denominator in Eq.(2) go to zero in the region, the projection requires a careful treatment and is much affected by unimportant

tails. However, we do not know the *real* three-particle distribution which should be used as a weight. Therefore we use Eq.(13) instead. We checked the most important quantity  $\omega = r_3(0)/2$  does not depend on a choice of the weight.

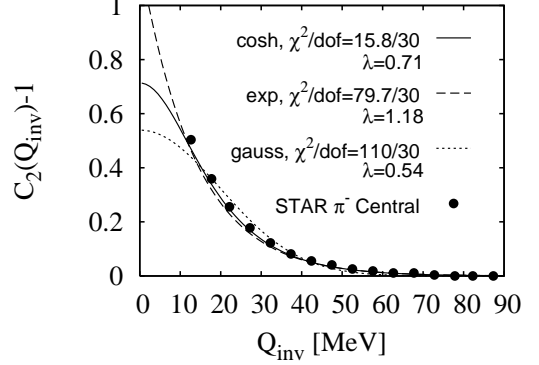


FIG. 1: Two-pion correlation function  $C_2(Q_{\text{inv}})$ . The lines denote our results of the fits for each source function. Closed circles stand for the experimental results.

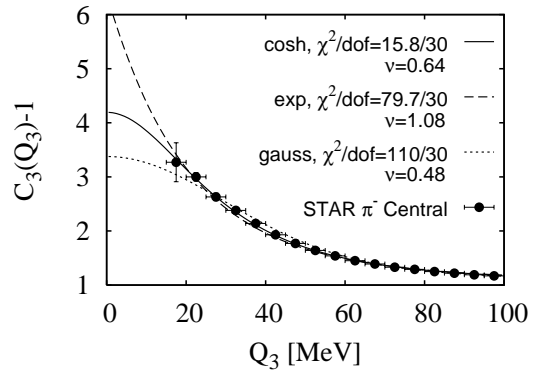


FIG. 2: Three-pion correlation function  $C_3(Q_3)$ . Each of symbols is similar to Fig. 1.

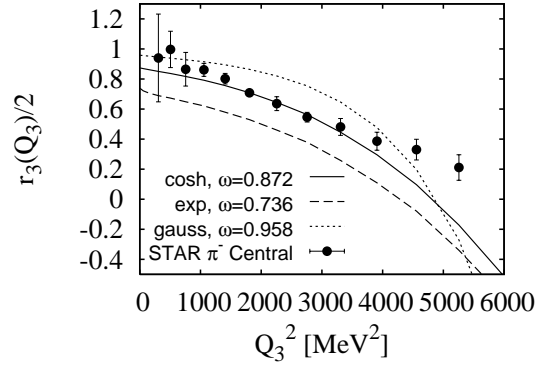
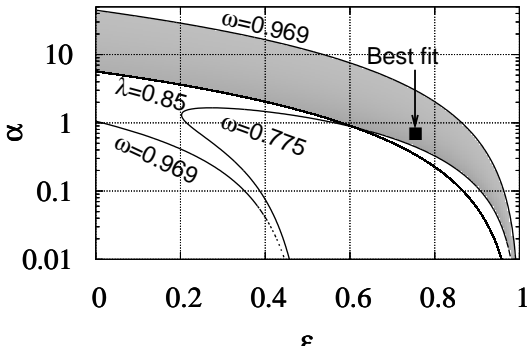


FIG. 3:  $Q_3$  dependence of  $r_3/2$ . Each of symbols is similar to Fig. 1 and 2.

Now let us evaluate how chaotic the pion sources are by using the models [Eqs. (3)-(6)] for the obtained  $\lambda^{\text{true}} = 0.93 \pm 0.08$  and  $\omega = 0.872 \pm 0.097$ , where we adopt the

TABLE II: Results for model I and II

	Model I	Model II
From $\lambda$	$\varepsilon_{pc} = 0.73 \pm 0.14$	$\alpha_m = 12.6 \pm 14$
From $\omega$	$\varepsilon_{pc} = 0.65 \pm 0.11$	$\alpha_m = 7.6 \pm 9.7$

FIG. 4: Results for the model III. Filled area is allowed parameter region for  $\alpha$  and  $\varepsilon$ . The filled square stands for the best fit point.

result of the  $\cosh$  source function. Allowed parameter regions of the Model I and II are summarized in the table II. Note that our calculation gives consistent results in each of the models. Huge uncertainty on  $\alpha_m$  is due to rapid changes of  $\alpha_m$  with  $\lambda$  and  $\omega$  around these parameter regions.

Allowed region of  $\varepsilon$  and  $\alpha$  of the model III is displayed in Fig. 4. In this figure, the filled area shows the ranges of  $\varepsilon$  and  $\alpha$  which correspond to the parameter region of the  $\lambda$  and the  $\omega$  estimated from the experimental data, respectively. The best fit point,  $\varepsilon = 0.75$  and  $\alpha = 0.77$ , is indicated by the filled square. Unfortunately, the uncertainty is still too large to give strong constraints on the pion production mechanism. Nevertheless, the result shows a strong correlation between  $\alpha$  and  $\varepsilon$ , that is, the experimental data show a mostly chaotic source which allows both “partial coherent” picture ( $\alpha \sim 0, \varepsilon \sim 1$ ) and “multicoherent” picture ( $\alpha \gg 1, \varepsilon \sim 0$ ). Though the fully chaotic source,  $\varepsilon = 1$ , is not excluded, the strong  $Q_3$  dependence of  $r_3(Q_3)$  in Fig. 3 is hardly reproduced by chaotic and symmetric sources. Even if the source is perfectly chaotic, asymmetry of the source could make a strong  $Q_3$  dependence. In this case, however,  $r_3$  becomes almost unity at small  $Q_3$ , while it deviates from unity at large  $Q_3$  [11]. Hence, at least, small coherent components are more likely to be produced.

In summary, we have given analyses of the three-pion correlation data by STAR together with the two-pion correlation in terms of three kinds of partial coherent source models. We found that all three models give consistent description for both three- and two-pion correlation if we

take account of the apparent reduction of the chaoticity in the two-pion correlation function caused by the long-lived resonance decays. All models give a consistent picture that pion emission in the RHIC experiment is mostly chaotic and coherent components are likely to exist (Table II and Fig.4). A further interesting problems on the multiplicity or collision energy dependence of the chaoticity will be published somewhere else [22].

The authors would like to acknowledge Profs I. Ohba and H. Nakazato for their support of this work. This work is partially supported by the Ministry of Education, Science and Culture, Japan (Grant No.13135221) and Waseda University Grant for Special Research Projects No. 2003A-095 and 2003A-591.

\* Electronic address: morita@hep.phys.waseda.ac.jp  
 † Electronic address: muroya@yukawa.kyoto-u.ac.jp  
 ‡ Electronic address: naka@hep.phys.waseda.ac.jp

- [1] B. Tomášik and U. A. Wiedemann, hep-ph/0210250.
- [2] Y. Hama and S. S. Padula, Phys. Rev. D **37**, 3237 (1988).
- [3] K. Morita, S. Muroya, H. Nakamura, and C. Nonoka, Phys. Rev. C **61**, 034904 (2000).
- [4] M. Gyulassy and S. S. Padula, Phys. Lett. B **217**, 181 (1988).
- [5] J. Bolz, U. Ornik, M. Plümer, B. R. Schlei, and R. M. Weiner, Phys. Rev. D **47**, 3860 (1993).
- [6] T. Csörgő, B. Lörstad, and J. Zimányi, Z. Phys. C **71**, 491 (1996).
- [7] H. Heiselberg, Phys. Lett. B **379**, 27 (1996).
- [8] U. A. Wiedemann and U. Heinz, Phys. Rev. C **56**, 3265 (1997).
- [9] M. Biyajima, A. Bartl, T. Mizoguchi, N. Suzuki, and O. Terazawa, Prog. Theor. Phys. **84**, 931 (1990).
- [10] U. Heinz and Q. H. Zhang, Phys. Rev. C **56**, 426 (1997).
- [11] H. Nakamura and R. Seki, Phys. Rev. C **60**, 064904 (1999).
- [12] H. Nakamura and R. Seki, Phys. Rev. C **61**, 054905 (2000).
- [13] J. Adams et al. (STAR Collaboration), Phys. Rev. Lett. **91**, 262301 (2003), nucl-ex/0306028.
- [14] H. Nakamura and R. Seki, Phys. Rev. C **66**, 027901 (2002).
- [15] P. Braun-Munzinger, D. Magestro, K. Redlich, and J. Stachel, Phys. Lett. B **518**, 41 (2001).
- [16] W. Broniowski and W. Florkowski, Phys. Rev. Lett. **87**, 272302 (2001).
- [17] The slightly larger  $\mu_B$  than previous analyses comes from larger  $\bar{p}/p$  value in the revised experimental data, C. Adler et al. (STAR Collaboration), Phys. Rev. Lett. **90**, 119903(E) (2003).
- [18] J. Cleymans and K. Redlich, Phys. Rev. C **60**, 054908 (1999).
- [19] C. Adler et al. (STAR Collaboration), Phys. Rev. Lett. **87**, 082301 (2001).
- [20] J. Adams et al. (STAR Collaboration), nucl-ex/0311017.
- [21] M. M. Aggarwal et al. (WA98 Collaboration), Phys. Rev. Lett. **85**, 2895 (2000).
- [22] K. Morita, S. Muroya, and H. Nakamura, in preparation.